Functionalization of Carbon Nano-onions by Direct Fluorination

Yu Liu,[†] Randy L. Vander Wal,[‡] and Valery N. Khabashesku*,[†]

Department of Chemistry and Richard E. Smalley Institute for Nanoscale Science and Technology, Rice University, 6100 Main Street, Houston, Texas 77005-1892, and The National Center for Microgravity Research at NASA-Glenn Research Center, Cleveland, Ohio 44135

Received September 12, 2006. Revised Manuscript Received October 30, 2006

Carbon nano-onions (CNO) are made of concentric fullerene-like shells and range from double- and triple- to multilayered structures. They remain the least studied allotrope of carbon yet. In the present study, a one-step process for functionalization of CNO (50−100 nm diameter) by addition of fluorine through direct fluorination at variable temperatures is reported. The reactions of CNO at three different temperatures, 350, 410, and 480 °C, yield fluorinated nano-onions (F-NO) of approximately $C_{10.1}F$, $C_{3.3}F$, and $C_{2.3}F$ stoichiometry, respectively, representing a new family of nanoscale fluorocarbon materials. The F-NO were characterized by a set of materials characterization methods including FTIR, Raman, UV−vis, and X-ray photoelectron spectroscopy, scanning (SEM) and transmission electron microscopy (TEM), X-ray diffraction, and thermal gravimetric analysis. SEM and TEM images show that even after breaking of the graphene layers in CNO by fluorine, the F-NO products retain the spherical onion-shaped morphology. The subsequent defluorination of F-NO by hydrazine treatment results in remarkable "healing" of broken graphene layers which rejoin within the sphere to substantially restore the CNO microstructure. In comparison with pristine CNO, fluorinated nano-onions show dramatically improved solubility in organic solvents, e.g., alcohols and DMF, enabling their processing for lubricating coatings, paints, nanocomposites, and biomedical applications.

Introduction

Since the discovery of buckminsterfullerene,[1] carbon-based nanostructures[2] became the hottest research topic in nanoscience. The ability of carbon to exist in several allotropic forms capable of creating a variety of nanoscale size shapes, such as spheres, tubules, onions, ribbons, and rods, provides fertile ground for many research efforts. In the past decade most studies on carbon nanostructures have focused on fullerene C_{60} as well as carbon nanotubes due to their unique electronic and mechanical properties[3−4] and potential applications in electronic devices,[5] polymer composites,[6−7] and hydrogen storage systems.[8] In contrast, carbon nano-onions (CNO), built of concentric fullerene-like shells that range from double- and triple-shelled to multilayered structures, remain the least studied allotrope of carbon so far. They began to become an attractive research target in 1992 when Ugarte discovered the transformation of carbon nanotubes into a new carbon material, carbon nano-onions, under intense electron-beam irradiation in a high-resolution electron microscope.[9] A number of synthetic methods to produce CNO in relatively high yields have been demonstrated thereafter, including arc discharge,[10−11] high-energy electron-beam irradiation,[9] high-temperature nanodiamond annealing,[12] plasma-enhanced chemical vapor deposition,[13] and implantation of carbon ions onto metal particles.[14]

Carbon nano-onions were already shown to offer a variety of potential applications including optical limiting,[15] solar cells, field emission,[16] and fuel cell electrodes.[17] New avenues for CNO uses can be proposed based on ability of filling the cavities in their hollow nanostructures with nanoparticles, which are expected to enable potential applications ranging from nanomagnets to systems for easy handling and protection of air-sensitive materials.[18,19] The unique graphitic

* To whom correspondence should be addressed. E-mail: khval@rice.edu.
[†] Rice University.
[‡] NASA-Glenn Research Center.

(1) Kroto, W. H.; Heath, J. R.; O'Brien, S. C.; Curl, R. F.; Smalley, R. E. *Nature* **1985**, *318*, 162.
(2) Shenderova, O. A.; Zhirnov, V. V.; Brenner, D. W. *Crit. Rev. Solid State Mater. Sci.* **2002**, *27*, 227.
(3) Dresselhaus, M. S.; Dresselhaus, G.; Eklund, P. C. *Science of Fullerenes and Carbon Nanotubes*; Academic Press: San Diego, CA, 1996.
(4) Ajayan, P. M. *Chem. Rev.* **1999**, *99*, 1787.
(5) Tans, S. J.; Verschueren, A. R. M.; Dekker, C. *Nature* **1998**, *393*, 49.
(6) Gong, X.; Liu, J.; Baskaran, S.; Voise, R. D.; Young, J. S. *Chem. Mater.* **2000**, *12*, 1049.
(7) Zhu, J.; Kim, J.; Peng, H.; Margrave, J. L.; Khabashesku, V. N.; Barrera, E. V. *Nano Lett.* **2003**, *3*, 1107.
(8) Liu, C.; Fan, Y. Y.; Liu, M.; Cong, H. T.; Cheng, H. M.; Dresselhaus, M. S. *Science* **1999**, *286*, 1127.
(9) Ugarte, D. *Nature* **1992**, *359*, 707.
(10) Sano, N.; Wang, H.; Alexandrou, I.; Chhowalla, M.; Teo, K. B. K.; Amaratunga, G. A. J.; Iimura, K. *J. Appl. Phys.* **2002**, *92*, 2783.
(11) Saito, Y.; Yoshikawa, T.; Inagaki, M.; Tomita, M.; Hayashi, T. *Chem. Phys. Lett.* **1993**, *204*, 277.
(12) Kuznetsov, V. L.; Chuvilin, A. L.; Butenko, Y. V.; Malkov, I. Y.; Titov, V. M. *Chem. Phys. Lett.* **1994**, *222*, 343.
(13) Chen, X. H.; Deng, F. M.; Wang, J. X. Yang, H. S.; Wu, G. T.; Zhang, X. B. *Chem. Phys. Lett.* **2001**, *336*, 201.
(14) Cabioch, T.; Riviere, J. P.; Delafond, J. *J. Mater. Sci.* **1995**, *30*, 4787.
(15) Koudoumas, E.; Kokkinaki, O.; Konstantaki, M.; Couris, S.; Korovins, S.; Detkov, P.; Kuznetsov, V.; Pimenov, S.; Pustovoi, V. *Chem. Phys. Lett.* **2002**, *357*, 336.
(16) Choi, M.; Altman, I. S.; Kim, Y. J.; Pikhitsa, P. V.; Lee, S.; Park, G. S.; Jeong, T.; Yoo, J. B. *Adv. Mater.* **2004**, *16*, 1721.
(17) Wang, H.; Abe, T.; Maruyama, S.; Iriyama, Y.; Ogumi, Z.; Yoshikawa, Z. *Adv. Mater.* **2005**, *17*, 2857.
(18) McHenry, M. E.; Subramoney, S. *Fullerenes: Chemistry, Physics and Technology*; John Wiley: New York, 2000.
(19) Subramoney, S. *Adv. Mater.* **1998**, *10*, 1157.

10.1021/cm062177j CCC: $37.00
Published on Web 01/26/2007

multilayer morphology also makes CNO materials very attractive candidates for studies of tribological friction and wear properties. It was established that the lubricating property of commonly used solid lubricants, e.g., graphite and molybdenum disulphide (MoS_2), is mainly attributed to their layered structure. They can form a thin layer between rubbing surfaces that shears easily and prevent contact between surfaces, thereby reducing friction and wear of the surfaces.[20] Theoretical and experimental studies suggest that cagelike nanoparticles with spherical or tubular structure can provide even greater application advantages in the tribology field.[21] With the graphitic layer-by-layer structures, carbon nano-onions are expected to be suitable for solid lubrication due to their nanometer-scale quasi-spherical shape, perfectly arranged outer shell, and stability.[22] CNO are also large enough to meet the rubbing surfaces asperity requirements and should possess adequate mechanical properties. Their advantage over graphite is that they have no edges where chemical attack can occur while maintaining the thermal stability of graphite.

Based upon tribology behavior of CNO, their use as potential additives in lubricating oil for aerospace applications in air environment has been proposed.[23]

Our recent studies of the related fullerene/graphene nanostructures, e.g., single-walled carbon nanotubes (SWNT), show that surface modification through chemical treatment, e.g., fluorination, can significantly affect their friction properties[24] as well as bring improvement in solubility in polar solvents and increase the chemical reactivity of SWNT, enabling a variety of functionalization reactions.[25−27] These studies also demonstrate the potential of chemistry on curved graphene surface as opposed to planar graphite. Therefore, exploration of chemical functionalization of CNO is attractive from both the fundamental chemistry and applications standpoints.

The number of published works on functionalization of CNO is still very sparse. The functionalization schemes described so far involve 1,3-dipolar cycloaddition chemistry[28,29] and derivatization of free carboxyl groups created on CNO surface through oxidative treatment by HNO_3.[29] These reactions were carried out on relatively small size CNO (not larger than 20 nm in diameter) and led to preparation of solubilized CNO. Functionalization of larger diameter CNO by addition reactions presents a challenge due to a lower surface curvature, which reduces the chemical reactivity. In the present work, we report a one-step process for functionalization of carbon nano-onions by addition of fluorine through direct fluorination at variable temperatures. The corresponding structure and property changes in the CNO caused by fluorination are discussed.

Experimental Section

Materials. The carbon nano-onions used in the present work were received in a powder form.[30] The CNO powder was made from carbon black by a proprietary inductive heating batch method that produces very high purity material in large quantities with CNO diameters ranging from 50 to 100 nm. Direct fluorination of CNO was carried out by using the fluorine (10%)−helium (90%) gas mixture purchased from Spectra Gases. Hydrazine of 97% purity was obtained from Aldrich.

Fluorination Procedure. The fluorination of CNO was carried out in a custom-built fluorination apparatus described elsewhere.[31] In a typical fluorination process, 200 mg of carbon nano-onions was loaded into a Monel-foil boat and then placed into a Monel reactor. Thereafter, the reactor was sealed and purged by continuous flow of helium for 2 h at room temperature and then under heating to reaction temperature. The reactor was heated to a selected temperature of 350, 410, or 480 °C. The sample was kept at that temperature for 2−3 h to remove the residual air and moisture adsorbed on the samples and reactor walls before fluorine and hydrogen were introduced into the reactor. Fluorine and hydrogen gases were introduced separately at a controlled 3:1 flow rate ratio. The purpose of using hydrogen in the process is in situ generation of HF, which is known to catalyze the fluorination of the other sp^2-bonded carbon materials, e.g., graphite and carbon nanotubes.[25] The fluorination time was kept at 6 h. Thereafter, the reactor was cooled down to room temperature, and the flows of hydrogen and fluorine gases were stopped. The sample weight was observed to increase from 200 mg to 231, 369, and 450 mg after the fluorination at temperatures of 350, 410, and 480 °C, respectively.

Hydrazine Treatment. In a typical procedure, 125−165 mg of fluorinated CNO powder and 25 mL of hydrazine were mixed together and sonicated for 1.5 h. An exothermic reaction producing white HF fume started almost immediately. The reaction proceeded most vigorously for the CNO sample having the highest fluorine content. The resulting hydrazine solution, containing the reaction products, was diluted with isopropanol and then filtered onto a 0.2-μm pore size PTFE membrane (Cole Palmer) to leave a deposit which was washed with isopropanol and then dried in a vacuum oven at 70 °C overnight. Depending on the fluorine content in fluorinated CNO, this procedure yielded 52−82 mg (60−85% theory) of black-colored all-carbon powder.

Characterization. The FTIR, UV−Vis, SEM/EDX, XRD, XPS, Raman, TGA, and TEM methods were used for characterization of pristine and fluorinated carbon nano-onion samples. The FTIR spectral measurements were performed using a Thermo Nicolet Nexus 670 FTIR spectrometer. The transmission mode IR spectra were collected from CNO samples (2.5 mg) mixed with the KBr salt (50 mg) and pressed into pellets. UV−vis spectra were obtained using a Cary 5000 UV−vis−NIR spectrophotometer. Scanning electron microscopy (SEM) was performed at 30 kV beam energy using a Phillips XL-30 field emission microscope equipped with

(20) Francis, J. C. *Solid Lubricants and Self-Lubricating Solids*; Academic Press: New York, 1972.
(21) Tenne, R.; Homyonfer, M.; Feldman, Y. *Chem. Mater.* **1998**, *10*, 3225.
(22) Hirata, A.; Igarashi, M.; Kaito, T. *Tribol. Int.* **2004**, *37*, 899.
(23) Street, K. W.; Marchetti, M.; Vander Wal, R. L.; Tomasek, A. J. *Tribol. Lett.* **2004**, *16*, 143.
(24) Vander Wal, R. L.; Miyoshi, K.; Street, K. W.; Tomasek, A. J.; Peng, H.; Liu, Y.; Margrave, J. L.; Khabashesku, V. N. *Wear* **2005**, *259*, 738.
(25) Khabashesku, V. N.; Billups, W. E.; Margrave, J. L. *Acc. Chem. Res.* **2002**, *35*, 1087.
(26) Khabashesku, V. N.; Margrave, J. L. Chemistry of Carbon Nanotubes. In *Encyclopedia of Nanoscience and Nanotechnology*; Nalwa, H. S., Ed.; American Scientific Publishers: Stevenson Ranch, CA, 2004; Vol. 1, p 849.
(27) Khabashesku, V. N.; Pulikkathara, M. X. *Mendeleev Commun.* **2006**, 61.
(28) Georgakilas, V.; Guildi, D. M.; Signorini, R.; Bozlo, R.; Prato, M. *J. Am. Chem. Soc.* **2003**, *125*, 14268.
(29) Rettenbacher, A. S.; Elliott, B.; Hudson, J. S.; Amirkhanian, A.; Echegoyen, L. *Chem. Eur. J.* **2005**, *11*, 1.
(30) Vander Wal, R. L.; Tomasek, A. J.; Street, K. W.; Hull, D. R.; Thompson, W. K. *Appl. Spectrosc.* **2004**, *58*, 230.
(31) Lu, Y. Ph.D. Thesis, Rice University, Houston, TX, 2005.

an energy dispersive X-ray (EDX) analyzer. X-ray diffraction data were collected on a GADDS powder diffractometer equipped with a Cu Kα radiation source. XPS data were obtained with a PHI Quantera X-ray photoelectron spectrometer using the monochromatic Al Kα radiation source (1486.6 eV) with a power setting of 350 W and an analyzer pass energy of 23.5 eV. The Raman spectra were collected with a Renishaw 1000 microraman system operating with a 514-nm laser source. Thermal degradation analyses were done with a TA-SDT-2960 TGA-DTA analyzer. Transmission electron microscopy (TEM) images were obtained using a Phillips CM200 microscope operating at 200 keV and equipped with a Gatan image filter (GIF) for digital imaging at a nominal resolution of 0.14 nm.

Results and Discussion

Fluorination of Carbon Nano-onions. For studies of temperature effect on fluorination, the carbon nano-onions were fluorinated at three different temperatures (350, 410, and 480 °C). These reactions yielded fluoro nano-onion products denoted as F-NO-350, F-NO-410, and F-NO-480, respectively. The SEM/EDX elemental analysis of the CNO and F-NO materials gave the following atomic % contents: CNO, C (91.5), O (8.5); F-NO-350, C (83.7), O (8.1), F (8.2); F-NO-410, C (69.4), O (9.8), F (20.8); F-NO-480, C (61.7), O (11.3), F (27.0). From these data, the bulk C/F stoichiometry of the F-NOs produced was calculated: at 350 °C, $C_{10.2}F$; at 410 °C, $C_{3.3}F$; at 480 °C, $C_{2.3}F$. Virtually no weight gain was observed at temperatures below 350 °C during the same (6 h) reaction time, indicating lack of a fluorination reaction. In brief, the bulk F/C ratio in the produced F-NO materials was noticed to grow with the increase of fluorination temperature. The highest F/C ratio, about 0.43, was observed in F-NO prepared by fluorination of CNO at 480 °C. The color of F-NOs obtained by CNO fluorination at 350 and 410 °C did not change as compared to that of the starting material and remained black, while fluorination of CNO at 480 °C produced a gray-colored powder due to higher fluorine content in the product. This resembles the color changes observed for the products of fluorination of graphite under the same temperatures.[32,33]

Solubility of Fluorinated Nano-onions. We found that the pristine CNO forms a black-colored colloidal suspension in ethanol after 20−30 min sonication. The majority of the CNO material precipitated from the suspension within 10 days, leaving a gray-colored supernatant solution (Figure 1A). In contrast, the similarly prepared colloidal suspensions of F-NO materials in ethanol (Figures 1B−1D) were light green-colored and remained quite stable for a long time. For instance, even after 1 year the suspension solutions of the most fluorinated F-NO-410 and F-NO-480 samples do not show any visible precipitation (Figures 1C and 1D) and the F-NO-350 sample, containing fluorine predominantly on the onion's outer layer, shows only a minor precipitation (Figure 1B). These observations demonstrate the significantly improved solubility of CNO due to functionalization through direct fluorination, similar to nanodiamond[31,34] and carbon nanotubes.[25]

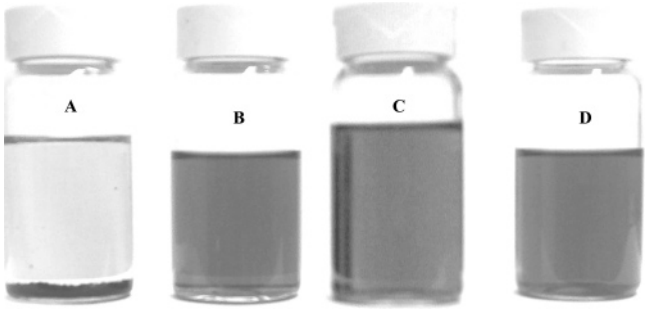

Figure 1. Photographs of the carbon nano-onion materials dispersion in ethanol: (A) pristine CNO, (B) F-NO-350, (C) F-NO-410, and (D) F-NO-480.

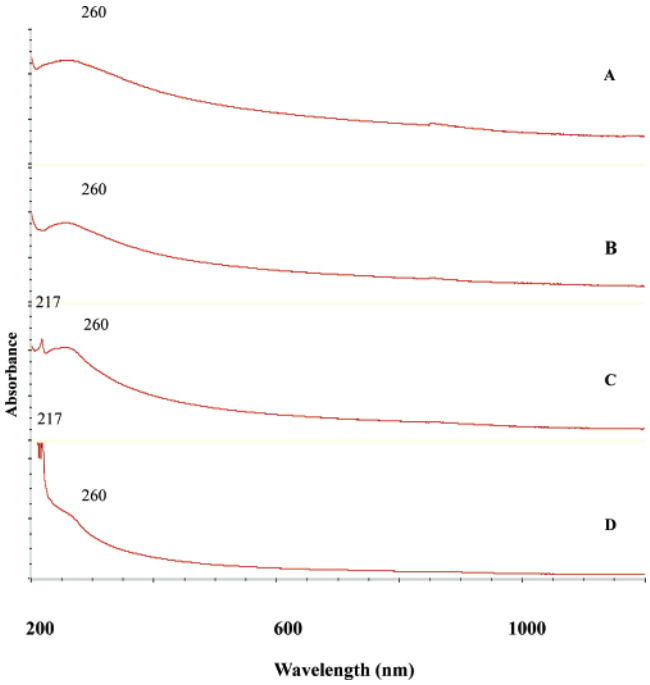

Figure 2. UV−vis spectra of pristine (A) and fluorinated carbon nano-onion samples at temperatures 350 °C (B), 410 °C (C), and 480 °C (D).

Characterization by Optical Spectroscopy. UV−vis spectroscopy serves as a probe for the effect of fluorination on π-bonded electronic configuration of carbon nano-onions being transformed from polyaromatic into polyene structures. UV−vis spectra of clear suspension solutions of CNO and F-NO samples in ethanol are shown in Figure 2. The spectrum of pristine CNO (Figure 2A) shows a single broad absorption peak at 260 nm, characteristic of $\pi-\pi^*$ electron transition in the polyaromatic system of curved graphite layers. The fluorination at 350 °C did not significantly change the optical absorbance features (Figure 2B) since at this temperature most likely only the outer layer of CNO has been modified by covalently added fluorine. Fluorination at higher temperatures, 410 and 480 °C, caused the appearance of an additional peak at 217 nm in the UV−vis spectrum of F-NO-410 (Figure 2C). This peak dramatically gains intensity in the spectrum of F-NO-480 while a broad band at 260 nm weakens (Figure 2D). The origin of this peak is most likely related to $\pi-\pi^*$ electron transitions in the polyene-type structures which are increasingly formed in F-NO with the

(32) Lagow, R. J.; Badachape, R. B.; Wood, J. L.; Margrave, J. L. *J. Chem. Soc., Dalton Trans.* **1974**, *12*, 1268.
(33) Kamarchik, P. Ph.D. Thesis, Rice University, Houston, TX, 1976.
(34) Lu, Y.; Gu, Z.; Margrave, J. L.; Khabashesku, V. N. *Chem. Mater.* **2004**, *16*, 3924.

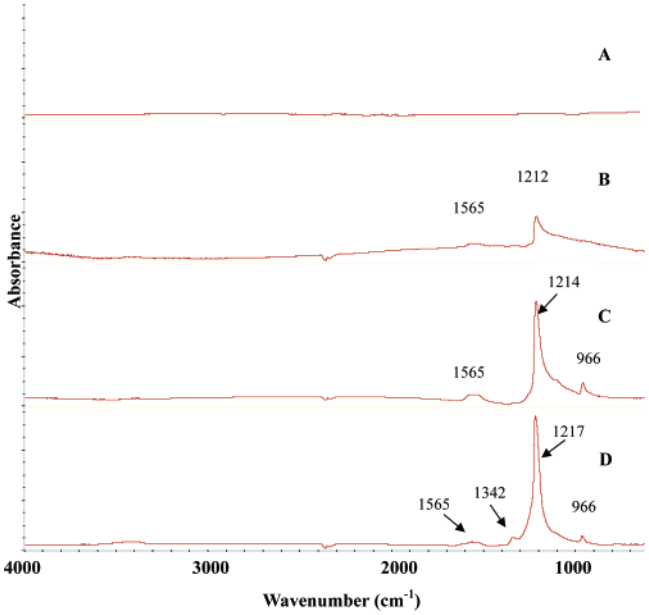

Figure 3. FTIR spectra of carbon nano-onions, pristine (A) and fluorinated at temperatures of 350 °C (B), 410 °C (C), and 480 °C (D).

growing extent of fluorination of inner graphitic layers under elevated temperatures.

The FTIR spectra of pristine carbon nano-onions and those fluorinated at three different temperatures are shown in Figure 3. The spectrum of pristine nano-onions is completely featureless, indicating no presence of IR-active functional groups in the CNO sample (Figure 3A). In the spectra of the fluoroproducts, fluorination of CNO leads to appearance of a dominant peak at about 1212−1217 cm^{-1} (Figure 3C,D) which belongs to the stretching vibrations of the tertiary C−F bonds[32] formed by covalent addition of fluorine to graphite-like layers in the CNO. The intensity of this peak is in-line with the fluorine content in the sample showing the highest peak intensity in the spectrum of F-NO-480 (Figure 3D). A weak absorption observed in the spectra of F-NO at about 1565 cm^{-1} is assigned to the vibrational mode of the "fluoroolefinic" C═C bonds which become IR-active due to breaking of the aromatic structure of the CNO through the addition of fluorine. The intensity of this peak decreases in the spectrum of F-NO-480 (Figure 3D) as compared to that of F-NO-410 (Figure 3C) due to a higher degree of fluorination of the C═C bonds. The other two weak bands observed at 966 and 1342 cm^{-1} (Figure 3C,D) can be assigned to the C−F stretching vibrations of the C═C−F and CF_2 moieties in the rings[35] located at the edges of nanosize segments formed by partial breaking of concentric graphitic layers in CNO during fluorination at temperatures higher than 400 °C.

Raman spectroscopy provides essential information for evaluation of the bonding states of carbons in the onion structure changed by fluorination. The Raman spectra collected for pristine and fluorinated CNO with different C/F stoichiometries are shown in Figure 4. In the Raman spectrum of pristine CNO (Figure 4A) a strong and sharp peak at 1582 cm^{-1} (G band) corresponds to the in-plane

(35) Roeges, N. P. G. *A Guide to the Complete Interpretation of Infrared Spectra of Organic Structures*; Wiley & Sons Publ.: New York, 1994.

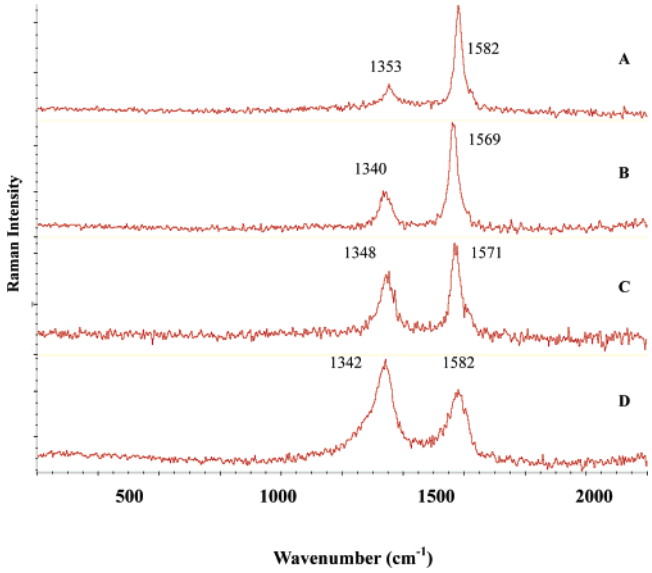

Figure 4. Raman spectra of pristine (A) and fluorinated carbon nano-onion samples: (B) F-NO-350, (C) F-NO-410, and (D) F-NO-480.

stretching vibration of the sp^2 carbon−carbon bonds within the ordered graphitic layers of CNO. A weaker peak at about 1353 cm^{-1} (D band) is related to the defects in the graphene structure. The D-band is also used as proof of the disruption of the aromatic system of π-electrons in the nano-onions framework due to the sp^3 states of carbon. The spectrum shown in Figure 4A suggests that the pristine nano-onions have an ordered structure with very few defect sites. In the Raman spectra of fluorinated samples (Figure 4B−D), the observed increase in intensity of the D band in the 1340−1348 cm^{-1} range indicates a rising abundance of the sp^3 bonded carbons in the F-NO structures due to fluorination. The addition of fluorine atoms to unsaturated carbon−carbon bonds changes the bonding configuration and overall symmetry in the onions. The G band is observed to weaken and broaden, which is related to a decreasing number of sp^2 bonded carbon atoms in the onion framework along with the growing disorder within layers. For the F-NO-480 sample, having highest F/C ratio, the Raman intensity of the sp^3 carbon related mode has surpassed that of the sp^2 mode (Figure 4D). This suggests that the fluorine addition has reached a certain level when most of the graphitic layers in the sample become modified into curved fluorographite-like structures of near C_2F stoichiometry.

X-ray Photoelectron Spectroscopy. The results of XPS surface analysis, which usually provide sampling at only a few nanometer depth of the solid, are in agreement with the optical spectroscopy data obtained for larger volume CNO specimen. In the XPS survey spectra, only a carbon peak was observed for the pristine CNO sample, while both carbon and fluorine peaks were detected for the fluorinated samples. The high-resolution spectrum of CNO shows a C 1s peak (Figure 5A) at 284.6 eV. This peak is located at exactly the same position as in the spectrum of graphite standard, confirming the polyaromatic graphitic structure of CNO built from C−C bonded carbons with sp^2 configuration. In the high-resolution C 1s spectrum of F-NO-350 sample, two peaks, attributed to two differently bonded types of carbons, were found (Figure 5B). The higher intensity peak, observed

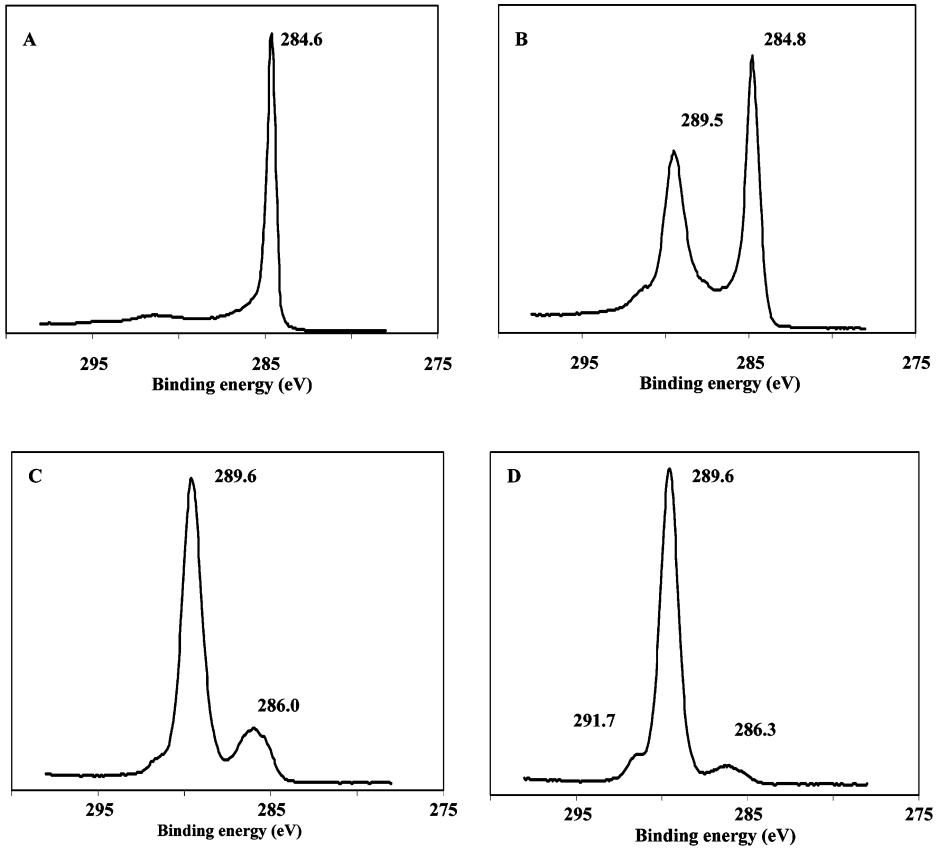

Figure 5. High-resolution XPS spectra of C 1s peak for pristine (A) and fluorinated carbon nano-onions at 350 °C (B), 410 °C (C), and 480 °C (D).

at 284.8 eV, characterizes the unfluorinated, yet polyaromatic, sp^2 carbons in the outermost surface layers of the sample. The lower intensity peak at 289.5 eV can be assigned to the sp^3 carbon atoms covalently bonded to fluorine by comparison with the known data on fluorinated graphite.[36−38] In the sample produced at a higher reaction temperature (410 °C) more fluorine is detected according to the XPS survey data. Two peaks are still observed in the high-resolution C 1s spectrum of F-NO-410 sample (Figure 5C). However, in this case the peak at higher energy (289.6 eV) becomes predominant due to the significantly increased number of sp^3 carbons bonded to fluorine. The increased fluorination also causes a shift in the position of peak originating from carbons bonded to fluorinated carbon to 286.0 eV (Figure 5C). Due to structural transformation of graphene layers in CNO under these conditions, the majority of carbons become polyene-type instead of being polyaromatic, as has been confirmed by observation of the C═C unit signatures in the UV−vis and FTIR spectra. In the C 1s spectrum of the sample fluorinated at the highest temperature (480 °C), the peak of these unfluorinated carbons weakens further due to addition of more fluorine to the carbons in the outer graphene layers than in the inner ones and shifts slightly further to 286.3 eV. Simultaneously, the peaks of carbons bonded to single fluorine (C−F moiety) and two fluorine atoms (CF_2 terminal group) at 289.6 and 291.7 eV, respectively, show a further increase in intensity due to a higher degree of fluorination of CNO. The calculated from XPS C 1s peak (Figure 5d) that elevated F/C composition, as compared to EDX analysis, most likely results from a nonuniform fluorination of graphene layers in CNO where several outermost layers add more fluorine than the majority of inner layers. The position of C 1s peak at 289.6 eV confirms the predominantly covalent nature of the C−F bond in F-NO since it is located very close to the C−F carbon peak position in the spectra of fluorographite C_2F[38] and multiwalled carbon nanotubes fluorinated at the same temperature. The observed positions of F 1s peak in the high-resolution XPS spectra of F-NO samples at 688.1−688.4 eV (not shown), which is far above the range for the ionic C−F bond (684−686 eV) and only slightly below the maximum value for the covalent C−F bond in PTFE (689 eV), provide further support for the near covalent character of the C−F bonding in F-NO.

Themal Gravimetric Analysis (TGA). The thermal degradation studies of CNO and F-NOs were carried out by the TGA method to obtain information on relative thermal stability of the materials with respect to fluorine content in the sample. The TGA experimental setup and run conditions were the same for all samples which were heated at a rate of 10 °C/min to 1000 °C in flowing air. The TGA plot in Figure 6A shows that pristine CNO material is stable in air up to a temperature of near 600 °C and quickly burns out within the temperature range of 625−700 °C. The least fluorinated sample, F-NO-350, already indicates a two-step weight loss on the TGA plot (Figure 6B). The first step weight loss of about 18 wt % takes place at temperatures

(36) Watanabe, N.; Nakajima, T.; Touhara, H. *Graphite Fluorides*; Elsevier: Amsterdam, 1988.
(37) *Fluorine-Carbon and Fluoride-Carbon Materials*; Nakajima, T., Ed.; Marcel-Dekker: New York, 1995.
(38) Nanse, G.; Papirer, E.; Fioux, P.; Moguet, F.; Tressaud, A. *Carbon* **1997**, *35*, 175.

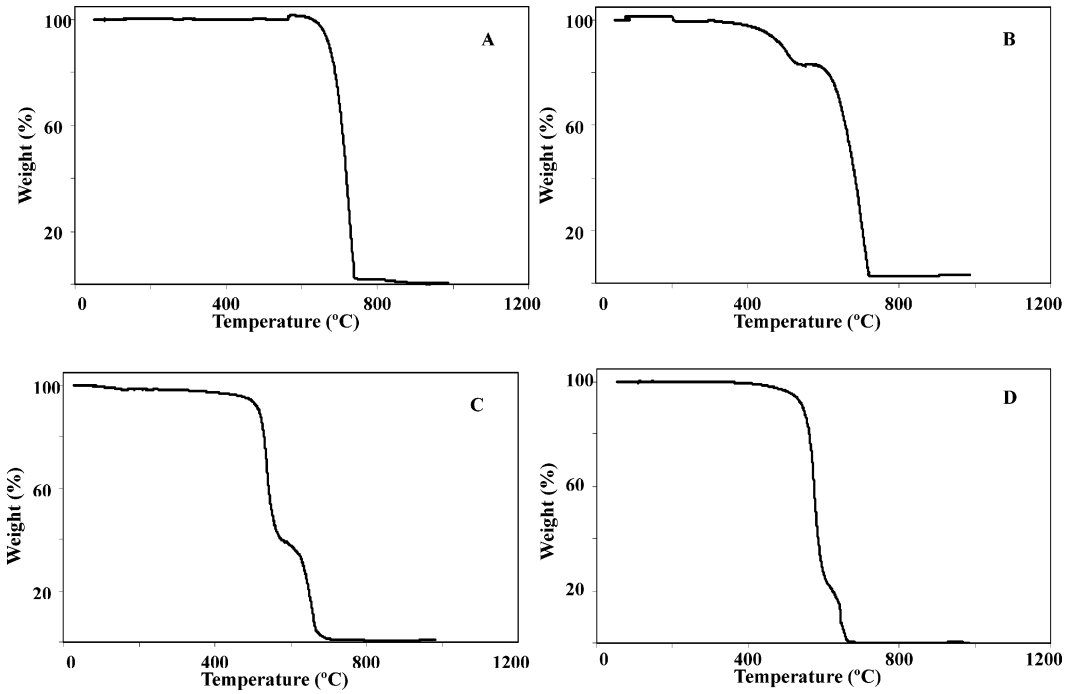

Figure 6. TGA weight loss plots in air for pristine (A) and fluorinated carbon nano-onion samples: (B) F-NO-350, (C) F-NO-410, and (D) F-NO-480.

between 430 and 550 °C and represents the oxidation and vaporization of outer fluorocarbon layers in the fluorinated onions. The second weight loss step is observed at the same temperature as for the pristine CNO, indicating a burnout of the inner all-carbon layers. The TGA plots obtained for higher fluorinated F-NO-410 and F-NO-480 samples are shown in Figures 6C and 6D. These plots also show the weight loss occurring in two steps; however, in comparison with F-NO-350 sample, the weight loss during the first step was observed to dramatically increase to 60 and 80 wt % for F-NO-410 and F-NO-480, respectively, due to oxidation and burning out of a greater number of fluorinated carbon layers. The second step weight loss of 40 and 20%, respectively, shown on these plots most likely relates to carbon in the inner core layers which remained unmodified by fluorine during fluorination of CNO at 410 and 480 °C, respectively. In summary, comparison of the TGA data on CNO and F-NO shows that the addition of fluorine to curved graphitic layers in CNO reduces the overall thermal stability of the onion structures.

Electron Microscopy Studies. The SEM images of pristine and fluorinated CNO samples are shown in Figure 7. The images show a quasi-spherical morphology for pristine nano-onion material with the particle sizes ranging from 30 to 100 nm in diameter (Figure 7A). Remarkably, the images of all fluorinated CNO samples (Figures 7B−7D) show no significant changes in particle shapes and sizes in comparison with the pristine CNO. This clearly indicates the strength of the nano-onion outer shell structure, which is capable of surviving even in the course of highly exothermic fluorination reaction. This helps to maintain an overall spherical morphology for F-NO materials.

High-resolution TEM enables closer imaging of the CNO microstructure and direct studies of the evolution of the curved graphite layers inside the onion spheres after exposure to fluorine at different temperatures. The selected HRTEM

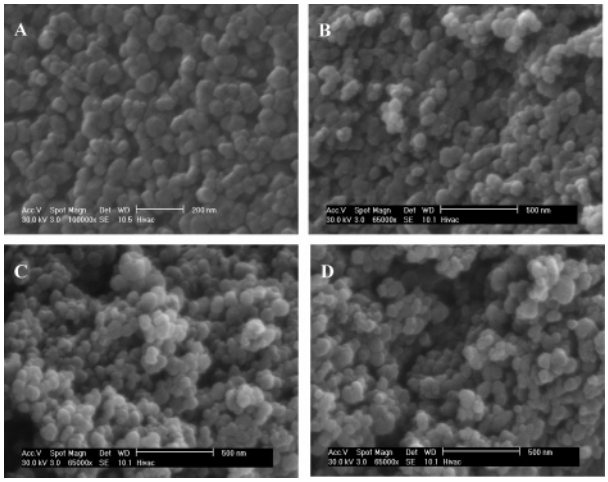

Figure 7. SEM images of carbon nano-onion samples taken before (A) and after fluorination at temperatures of 350 °C (B), 410 °C (C), and 480 °C (D).

images of pristine and fluorinated CNO samples are shown in Figure 8. Pristine CNO particles exhibit faceted microstructure consisting of parallel graphitic layer planes extending several tens of nanometers in each single onion (Figure 8A). The hollow interior in the onion is surrounded by multiple layers of nested concentric graphite shells that appear as dark lines representing the individual atomic layers. The fluorination process appears to disrupt the integrity of the graphene layers of the onions by starting from the outside and moving inward. The HRTEM image of F-NO-350 sample (Figure 8B) shows the outer layers that are altered up to a few nanometers depth. The interior structure of the nano-onions remains intact and still exhibits the ordered atomic layer planes. Notably, in some onions the interior is still preserved, indicating the contiguous nature of the graphene layers with no pores or breaks. Such preservation also speaks for the "sealed" nature of the onions, whereby the graphene layers are largely continuous and form a seal

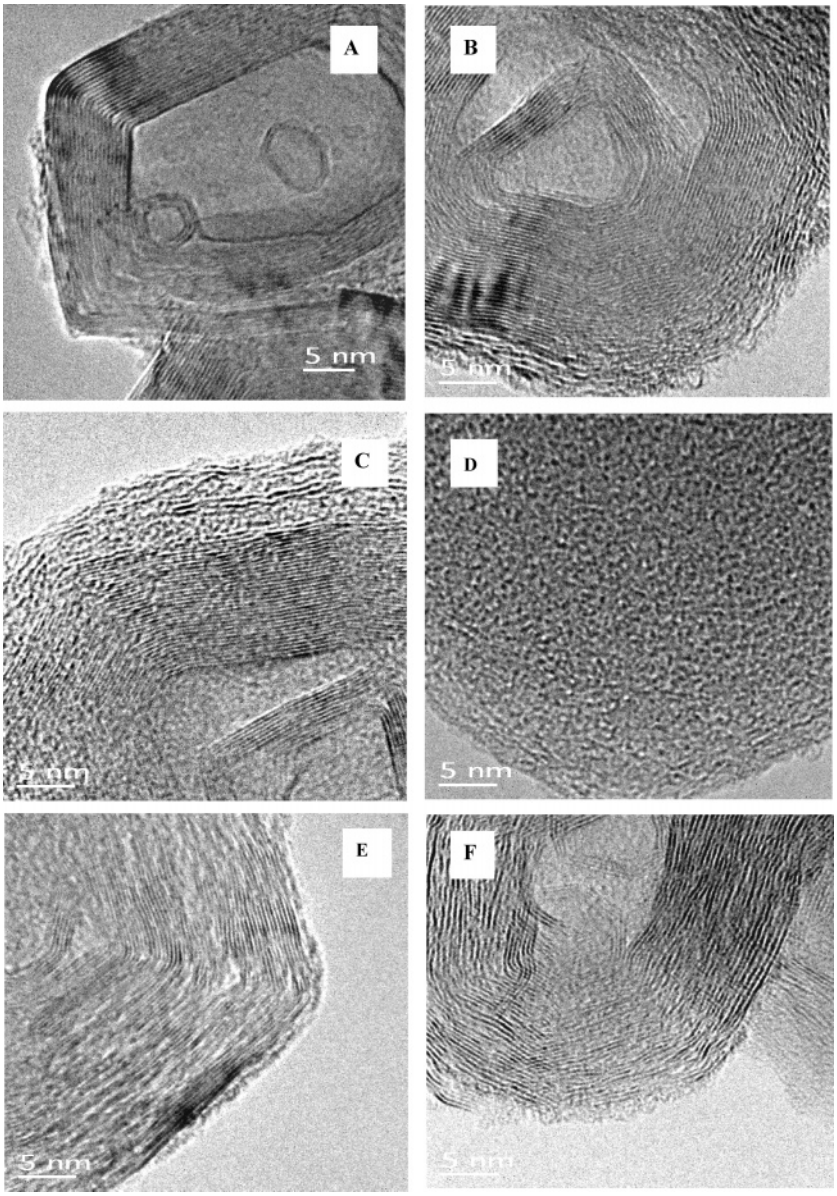

Figure 8. TEM images of carbon nano-onion specimens: (A) pristine CNO, (B) F-NO-350, (C) F-NO-410, and (D) F-NO-480; hydrazine-treated F-NO-410 (E) and F-NO-480 (F).

around the interior. This is also consistent with the high thermal stability of the onions.

Yet a higher degree of fluorination leads to a greater level of penetration into the onion with corresponding breakup and disruption of the ordered layers. The images of F-NO-410 and F-NO-480 (Figures 8C and 8D) show a deeper penetration of the fluorination process into the onion microstructure as seen by the greater depth of the shortened segments of fluorocarbon created from the graphitic lamella. The increase in the interlayer distances can also be observed. However, overall quasi-spherical morphology is still preserved. This is particularly demonstrated by the image of F-NO-480 sample (Figure 8D) where the formerly hollow interior becomes entirely filled with the randomly oriented very short fluorocarbon segments all confined within the outer shell.

Powder X-ray Diffraction Data. The XRD measurements also confirm that the layered structures of the nano-onions have been drastically altered due to fluorination. The X-ray diffraction patterns obtained for all samples in the 2θ range of $5°-90°$ are compared in Figure 9. As shown in Figure 9A, the analysis of pristine CNO yielded four peaks at $2\theta = 25.91$ (002), 42.55 (100), 53.64 (004), and 78.04 (110)° which are resembling the XRD patterns of graphitized carbon materials.[37,39] By application of Bragg's and Scherrer's equations, the average interlayer *d*-spacing and crystallite size in CNO were calculated to be 0.344 and 7.75 nm, respectively, which are characteristic of short-range ordered curved nanographite planes. In the course of fluorination at increasing temperatures, XRD peaks of CNO are observed to reduce and disappear (Figure 9B-D) with the increasing fluorine content, suggesting that fluorination gradually changes and finally disrupts all graphite layers inside the nano-onions at 480 °C. For the F-NO-350 sample the XRD peaks were found at almost the same positions as those for

(39) Pierson, H. O. *Handbook of Carbon, Graphite, Diamond and Fullerenes*; Noyes Publ.: Park Ridge, NJ, 1993.

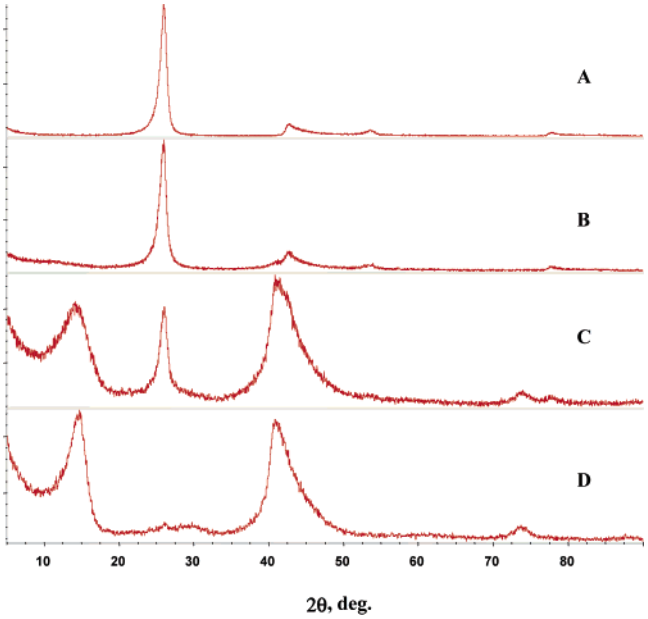

Figure 9. XRD patterns of carbon nano-onion samples: pristine (A) and fluorinated at 350 °C (B), 410 °C (C), and 480 °C (D).

pristine CNO (Figure 9B), corresponding to the interlayer distance $d(002) = 0.343$ nm and crystal size of 7.82 nm. Due to fluorination of only the outer layers in the onions, as indicated by TEM and C/F stoichiometry EDX data, only one additional low-intensity shoulder peak at $2\theta = 40.84°$ was detected for this sample. However, the XRD of F-NO-410 sample (Figure 9C) already shows a significant reduction in the intensity of peaks due to graphitic layers, separated by $d(002) = 0.341$ nm inside the onion shells, and appearance of new broad features at $2\theta = 14.16$, 40.86, and 73.96°. These reflections characterize the fluorocarbon layers that are broken into shorter segments, as shown by TEM (Figure 8C). The layers are separated by distance $d(002) = 0.625$ nm and give the average nanocrystal size of 1.76 nm calculated from the half-width of the XRD peak at $2\theta = 14.16°$. For the sample fluorinated at 480 °C, only the XRD peaks of virtually uniform fluorocarbon product are detected at $2\theta = 14.88$, 40.86, and 73.67° (Figure 9D). The corresponding calculated lattice distance $d(002)$ is 0.595 nm and the average crystal size of fluorocarbon segments is 4.4 nm. The fluorocarbon interlayer distances $d(002)$ observed through XRD for F-NO-410 and F-NO-480 onions are within the 0.555−0.660 nm range characteristic of C_nF ($n > 2$) fluorographite materials.[36]

Defluorination of F-NO through Hydrazine Treatment. Previous studies have shown that fluorinated nanocarbons, such as single-walled carbon nanotubes,[25,40] nanodiamond,[33,41] and graphite,[40] when treated with hydrazine H_2-NNH_2, undergo defluorination via the following reaction: $4C_nF + N_2H_4 \rightarrow 4C_n + 4HF + N_2$, providing a useful tool for chemical modification of carbon nanomaterials. To verify the applicability of this method to carbon nano-onions, the F-NO powders were also treated with hydrazine. We noticed that after the reaction the color of all treated FNO samples returned to black, indicating the graphitization of the surface due to elimination of fluorine. The FTIR spectra of hydrazine-treated samples appeared very similar to spectra of pristine CNO, showing no peaks due to C−F or any other groups. The SEM/EDX elemental analysis yielded fluorine content in these samples to be less than 1 at. %. These data as well as the high yields (60−85%) of all-carbon onion-like materials, obtained after filtering, washing, and drying the reaction products, also support the occurrence of defluorination. Furthermore, the TEM images of hydrazine-treated F-NO-410 and F-NO-480 samples (Figures 8E and 8F, respectively) confirm the removal of fluorine as well. This is indicated by the observed partial reforming of the layers, increase in the degree of ordering of graphene layers formed, and reduction of spacing between the layers. It is interesting to see that the hydrazine treatment also permits some "healing" of the broken graphene segments which join into ribbons or bands inside the particle perimeter. The bands shift in the direction from inside out, leading to the partial restoration of the hollow microstructure of the onions, as seen in Figure 8F. Degree of ordering is increased in addition to alignment, although with less crystalline perfection as for the original CNO material. Nevertheless, the overall shell-like morphology of the onions is once more preserved.

Conclusions

In this work we have shown that direct fluorination of carbon nano-onions (CNO) at three different temperatures, 350, 410, and 480 °C, produces fluorinated nano-onions (F-NO) of approximately $C_{10.1}F$, $C_{3.3}F$, and $C_{2.3}F$ stoichiometry, respectively. The high-temperature reaction conditions and high-frequency C−F stretch peak position in the IR spectra suggest a predominantly covalent bonding of fluorine to carbon in F-NO. The F-NO materials exhibit significantly improved solubility in organic solvents, such as alcohols and DMF, as compared to the pristine CNO. Improved solubility opens an opportunity for further functionalization of the F-NO by fluorine substitution reactions, by analogy with the similarly soluble fluorinated single-walled carbon nanotubes and nanodiamonds.[25,33] As a result, direct fluorination can be used as the first step in the organic functionalization of CNO for nanocomposites, paints, coatings, and biomedical applications.

SEM and TEM images show that even after the addition of fluorine to virtually all graphene layers the fluorinated products still retain the spherical onion-shaped morphology. The consecutive addition of fluorine breaks the graphene layers in CNO into short segments of just a few nanometers length which fill up the hollow interior of the onions in F-NO while the average outer size of the sphere is preserved. More remarkably, a subsequent hydrazine treatment not only readily defluorinates the F-NO but also causes a substantial "healing" of broken graphene layers which rejoin within the onion microstructure. This can serve as an interesting and unique example of nanoscale chemistry proceeding under confinement conditions and deserves further study.

(40) Mickelson, E. T. Ph.D. Thesis, Rice University, Houston, TX, 1998.
(41) Liu, Y.; Khabashesku, V. N.; Halas, N. J. *J. Am. Chem. Soc.* **2005**, *127*, 3712.

The fluorinated carbon nano-onions represent a new family of nanoscale fluorocarbon materials with a remarkably stable sphere-shaped multilayered morphology, making them very attractive candidates for application as lubricants. Work in progress in our laboratories involves tribology studies of friction and wear properties of these materials in air and inert environments, both in neat form and as additives to lubricating fluids. Studies of chemical functionalization of FNO through fluorine displacement are also underway.

Acknowledgment. This work was supported by The Robert A. Welch Foundation and in part by Award No. RUE2-2659-MO-05 of the U.S. Civilian Research & Development Foundation for the Independent States of the Former Soviet Union (CRDF). We thank Mr. William V. Knowles for assistance in collecting XRD data and Dr. V. A. Davydov for valuable comments on the manuscript.

CM062177J